



Third European Conference on the Structural Integrity of Additively Manufactured Materials
(ESIAM23)

Development of DED Process Parameters for Deposition of Bronze and Evaluation of Its Wear Properties under Dry Sliding Conditions.

Sunil Raghavendra^a, Sasan Amirabdollahian^b, Matteo Perini^b, Marco Chemello^c, Matteo Benedetti^{a*}

^aDepartment of Industrial Engineering, University of Trento, Trento 38123, Italy

^bProM Facility, Trentino Sviluppo S.p.A, Rovereto 38068, Italy

^cSicor S.R.L, Rovereto 38068, Italy

Abstract

With the Directed Energy Deposition (DED) process, we aim to develop an efficient way to reduce the use of bronze in worm gears. Due to the limited study conducted on the DED of bronze on steel substrate, optimizing the process parameters for a high-quality deposition is essential. Therefore, in the current study, we evaluate the effect of process parameters such as laser power, feed rate, and scanning speed on the deposition of Bronze on a 42CrMo4V substrate. Single bronze tracks were deposited using different laser power values, feed rates, and scanning speed. Cross-sections of the depositions were analyzed for porosity and track dimensions to obtain the aspect ratio. The best parameters from the single-track deposition were selected, and multiple-layer deposition was created for a thickness of 3 mm. Cylindrical specimens were extracted from this multilayer deposition and subjected to wear tests using the pin-on-disc configuration under dry sliding conditions against a 42CrMo4V counterface to check for debonding and friction behavior. The DED specimens were characterized for porosity, microstructure, and microhardness. Finally, the results, when compared with the properties of wrought Bronze, indicate that the DED bronze can be used as a replacement for wrought Bronze in gears.

© 2023 The Authors. Published by Elsevier B.V.

This is an open access article under the CC BY-NC-ND license (<https://creativecommons.org/licenses/by-nc-nd/4.0>)

Peer-review under responsibility of the scientific committee of the ESIAM23 chairpersons

Keywords: Direct Energy Deposition (DED); Bronze; Process parameters; Porosity; Wear

* Corresponding author. Tel.: +39-046-128-2457

E-mail address: matteo.benedetti@unitn.it

1. Introduction

Bronze, a copper-based alloy with approximately 10% tin content, is commonly used in the construction of worm gears, known for their high reduction ratios and compact designs (Fontanari et al. 2013). Worm gears, due to their complex geometry, extensive contact surfaces, and high sliding rates, benefit from bronze's properties, which act as a sacrificial element, adapting tooth geometry, damping shocks, and serving as a solid lubricant during cold start-ups (Crosher 2002). However, as bronze relies on copper, a critical raw material with increasing costs attributed to electrification and environmental regulations, there is a growing interest in innovative solutions for more efficient material usage. Additive manufacturing (AM) techniques, such as laser-directed energy deposition (L-DED), might be one of the solutions as it offers the potential to create complex shapes and repair using multi-material in 3D (Maconachie et al. 2019; Benedetti et al. 2021). L-DED involves depositing metal powder or wire onto a substrate while simultaneously heating it, typically in an inert atmosphere to prevent oxidation. Apart from the ability to use multiple materials in a single component and create complex shapes, the rapid build rate makes it an efficient process (Ahn 2021; Dávila et al. 2020). However, challenges arise when applying AM to copper and its alloys, including issues related to reflectivity and thermal conductivity, which can lead to unmelted zones porosity and can threaten the optics of the machine (Yadav, Paul, et al. 2020; Emminghaus et al. 2019; Müller et al. 2021).

Additive manufacturing (AM) processes have significantly advanced our understanding of the mechanical characteristics of various metals, primarily concentrating on their static and fatigue performance. However, research into the wear and tribological properties of these metals has predominantly centered on specific conventional AM materials. For instance, Prashanth et al. (Prashanth et al. 2014), investigated the wear characteristics of Al-Si alloy manufactured using the SLM process and concluded that as-built material had better wear performance compared to annealed AM specimens. AM manufactured stainless steel was tested for wear properties at different temperatures (Duraisamy et al. 2020). Inconel 718 specimens manufactured using the DED process have been tested for wear properties for application in damage repair (Onuiké and Bandyopadhyay 2019). Ti64 and Fe-Cu specimens manufactured using the EBM process have also been investigated for their tribological behavior (Zykova et al. 2022; Bruschi et al. 2016).

The existing studies primarily utilize the SLM or DED process to deposit pure copper, bronze, or multi-material compositions and test them under static loading conditions. Given the outstanding wear and tribological properties of copper and its alloys, it becomes crucial to investigate the influence of AM process parameters on their wear and tribological characteristics. Our previous research (Raghavendra et al. 2023) focused on depositing CuSn10 with and without a buffer layer of CuSn10+316L between the deposition and the steel substrate and evaluating the effect of process parameters and the wear behaviour. The specimens showed inter and intra-layer porosity, which decreased with the presence of the buffer layer and the use of high laser power. The wear properties were also comparable to wrought bronze in this case.

The current study was conducted to further explore this domain of using DED for Cu alloys, for application in wear resistance coatings, and for efficient usage of bronze. The study focuses on assessing the deposition of CuSn12Ni2 (mentioned as bronze) alloy on a 42CrMo4V steel substrate using the DED method. The study was conducted starting from the process parameter characterization using single-track deposition, followed by multiple-layer deposition to extract pins for the Pin-on-Disc wear test. The specimens were characterized for porosity, microhardness, and microstructure to understand the effect of process parameters on the deposited bronze.

2. Materials and methods

2.1. Powder

The air-atomized bronze powder with a composition of CuSn12Ni2 and particle size distribution between 45 – 150 μm was obtained from Linbrazo S.r.l. The obtained powders were characterized using SEM and EDXS analysis to examine their composition and morphology. The powder particles slightly deviated from the spherical shape and some elongated particles were also observed, as shown in Fig. 1(a). The chemical composition obtained from the EDXS analysis is shown in Fig. 1(b) and tabulated in Table 1.

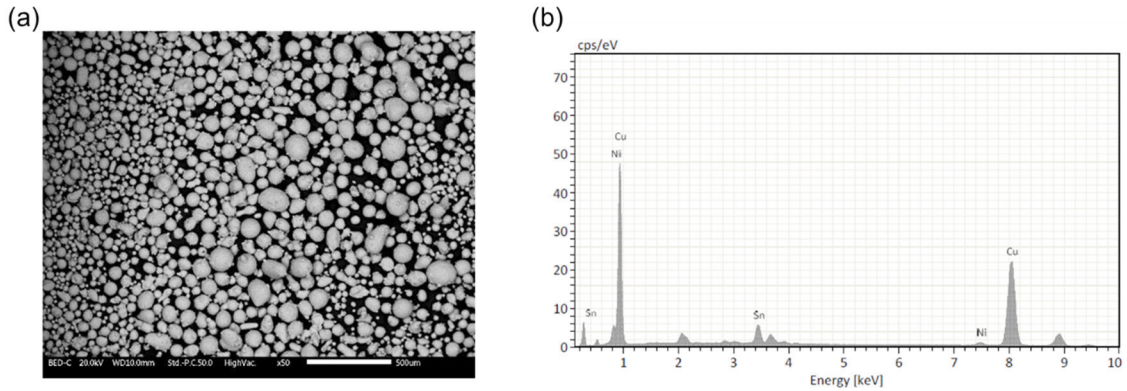


Figure 1 (a) SEM image of the powder particles (b) Chemical composition spectra of the powder from EDXS

Table 1 Elemental composition of the powder used for DED process

Element	Mass normalized (%)
Copper (Cu)	87.74 ± 0.12
Tin (Sn)	10.56 ± 0.14
Nickle (Ni)	1.69 ± 0.02

2.2. DED process parameters

The DED process of the bronze was carried out using a Lasertec 65 DED using a laserline diode with a maximum laser power of 2500 W, 3 mm coaxial nozzle with argon carrier gas. The deposition process of this study was conducted in two stages. An initial deposition on single tracks was carried out to evaluate the best parameters for the next stage of depositing multiple layers. The deposition was carried out on a 42CrMo4V substrate in both steps of the study.

2.2.1. Single-track deposition

Single tracks of 30 mm in length were deposited on the 42CrMo4V substrate. The deposition was carried out using a combination of parameters indicated in Table 1, and the carrier gas flow rate was maintained at 6 L/min. The deposited tracks were visually evaluated for any discontinuity during the deposition. The cross-section of the tracks was analyzed to obtain the aspect ratio and the porosity of the bead.

Table 2 DED process parameter for single-track deposition

Spot diameter (mm)	Laser power (W)	Scanning speed (mm / min)	Feed rate (g/min)	Carrier gas flow rate (L/min)
3	1000 – 2200	600 and 800	6 and 8	6

2.2.2. Multi-layer deposition

Based on the single-track deposition results discussed in section 3.1, the multi-layer specimens with five layers were obtained using the parameters indicated in Table 2. A bi-directional double pass pattern with 90° rotation for each

layer was used in the deposition process, with an overlap of 50% of the track width between the tracks. The deposition pattern in specimens 1 and 2, the laser power was decreased by 100 W for each layer, with the minimum laser power of 1700 W used for the top two layers. While for specimens 3 and 4, all five layers were deposited using 2000 W of laser power. Additionally, two different carrier gas flow rates were used for the deposition, as indicated in Table 2. A schematic of the top view of the multiple tracks is shown in Fig 2(a), the cross-section in Fig 2(b), and the pins extracted for the Pin-on-Disc test in Fig. 2(c),

Table 3 DED process parameters for multi-layer deposition

Spec No	Laser power (W)	Feed rate (g/min)	Scanning speed (mm/min)	No. of Layers	Carrier gas flow rate (L/min)	Laser power variation
1	2000	8	800	5	4.5	Decreasing
2	2000	8	800	5	6	Decreasing
3	2000	8	800	5	4.5	Constant
4	2000	8	800	5	6	Constant

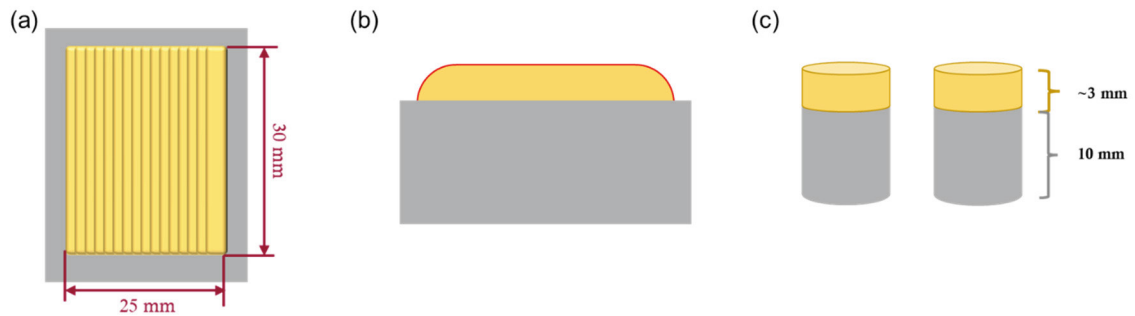


Figure 2 Schematic diagram of (a) top view of the deposition (b) cross-section of the multi-layer deposition and (c) cylindrical pins extracted for the Pin-on-Disc test

2.3. Porosity, microhardness and microstructure

The characterization was carried out to evaluate the deposition quality obtained from the DED process for single-track and multiple-layer specimens.

2.3.1. Porosity

It has been determined that the DED process parameters impact the pores within the samples. Therefore, to gain insights into how these parameters affect porosity, the cross-sections of single-track and multi-layer depositions were analysed. The specimens underwent a series of steps, including cutting, mounting, and polishing, using SiC abrasive papers with grit sizes ranging from 500 to 4000. Subsequently, the specimens were polished on cloth using diamond suspension solutions with particle sizes of 3 μm and 1 μm . Comprehensive images of the specimens were captured using a light optical microscope (LOM) and stereomicroscope in the case of multi-layered pins and subjected to analysis using ImageJ®. The percentage of porosity within the specimens was determined using Equation 1.

$$Porosity = \frac{\sum Area\ of\ pores}{Total\ area} \times 100 \quad (1)$$

2.3.2. Microhardness

The multi-layer specimens were subjected to microhardness testing using a Future tech FM-310 Vickers microhardness testing apparatus equipped with a diamond indenter. A load of 100 gf was applied, with a dwell time of 10 seconds. The specimens were segmented into five zones with an increment of 5 mm from the substrate. Each of these regions underwent five separate hardness measurements, and the hardness values were subsequently extracted directly using Alexasoft software. The microhardness measurements were compared with the wrought bronze.

2.3.3. Microstructure

Microstructure analysis was performed on the cross-section of the multi-layer specimens to examine how laser power influenced the type and size of grains in the microstructure. The polished specimens from the porosity analysis were utilized for this examination. The etching process was carried out using an iron (III) chloride etchant to uncover the microstructure of the bronze deposition.

2.4. Wear test

Wear testing was performed using the Ducom Pin-on-Disc testing machine, employing dry sliding conditions. The test involved subjecting DED Bronze pins to wear test against a 42CrMo4V steel counterface. The pins had a diameter of 10 mm at the deposition site following machining and a total height of 13 mm. The 42CrMo4V steel discs used were 7 mm thick and 63 mm in diameter. The tests were executed at room temperature, employing a sliding velocity of 1 m/s (300 RPM) for a duration of 60 minutes, maintaining a constant load of 0.5 MPa. At intervals of 10 minutes, the test was temporarily halted to look for consistency in their behaviour. All tests were conducted on new, polished discs. The primary objective of the Pin-on-Disc tests was to assess whether the specimens could endure the generated forces without experiencing any separation between the deposited bronze material and the steel substrate. In addition to the DED deposited pins, a wear test was also conducted on a wrought bronze pin to analyse for comparison of the friction coefficient.

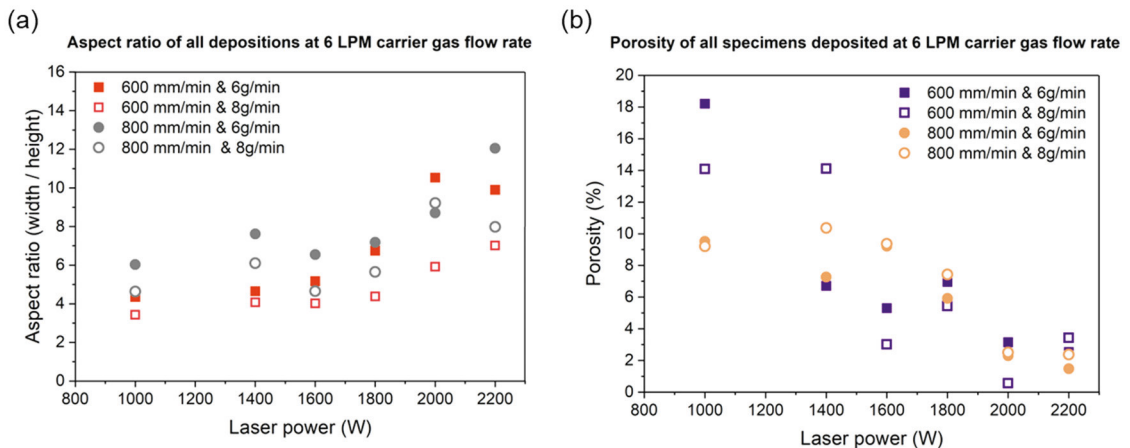


Figure 3 Effect of laser power on (a) aspect ratio of the bead (c) area porosity of the cross-section

3. Results and discussion

3.1. Single-track deposition

As mentioned in section 2.2.1, continuous single tracks of the bronze were deposited using a range of parameters. The cross-section of these tracks was analyzed to calculate the aspect ratio of the bead (track width/track height), observe the dilution of the substrate into the deposition, and the porosity of the bead using a Light Optical Microscope (LOM). As mentioned previously, the parameters that yielded satisfactory single tracks were used for the multi-layer deposition.


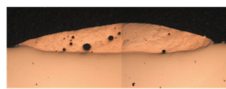
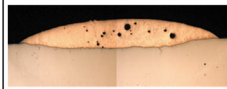
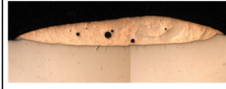
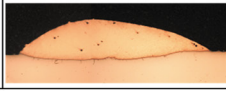

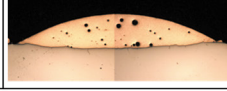
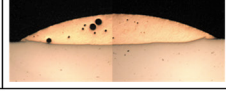
	2000 W		2200 W	
	600 mm/min	800 mm/min	600 mm/min	800 mm/min
6 g/min				
8 g/min				

Figure 4. Cross-section of single-track depositions at 2000 W and 2200 W laser power

The variation of aspect ratio with laser power is shown in Fig. 3(a). The bead geometry is mainly dominated by the deposition's laser power, followed by the feed rate, and scanning speed, which contribute to the amount of material available and the interaction time. As the laser power increases, the track width increases due to the formation of a larger melt pool at high laser power. In the case of track height, generally, a slight increase is observed with an increase in the laser power, but after a threshold, the height decreases due to the increase in the laser power per unit length of the deposition, leading to a larger melt pool. As seen in Fig. 3(a), the aspect ratio generally increases with an increase in the laser power. However, at 2200 W, for deposition at 600 mm/min and 6 g/min, and 800 mm/min and 8 g/min, we see a slight decrease in the aspect ratio. The aspect ratio values greater than five and less than eight yield an efficient multi-layer deposition with better overlap and considerably suitable thickness (Yadav, Paul, et al. 2020; Yadav et al. 2022; Yao et al. 2022; Paul et al. 2013). The track width and the height values obtained from the beads are used to deposit multiple layers in the next stage.

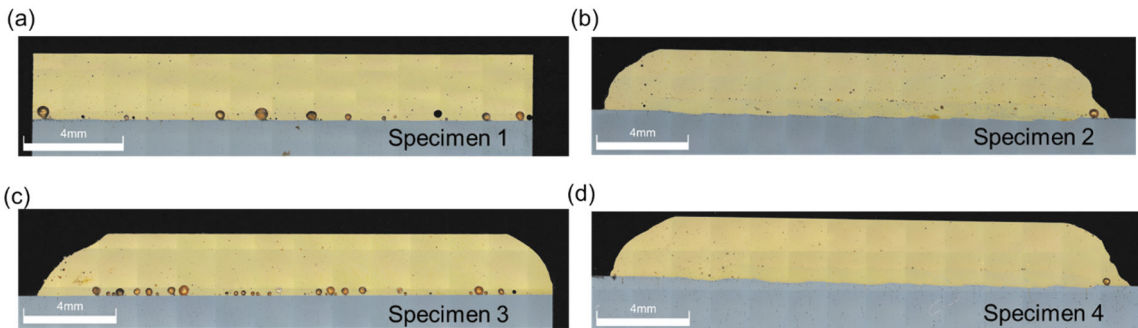


Figure 5 Cross-section of multi-layer deposition indicating the pore distribution in the specimens.

The porosity of the single-track beads was analyzed to select the parameters with the least porosity for multi-layer deposition. The effect of laser power on porosity is indicated in Fig. 3(b), a drastic decrease in porosity is observed with an increase in the laser power due to complete fusion of material. Porosity values less than 4% were noticed for

specimens deposited at 2000 and 2200 W laser power. The cross-section of the specimens with the least porosity is shown in Fig. 4.

Depending on the aspect ratio, dilution, porosity, and symmetry of the single-track bead, the parameter with 2000 W laser power, 800 mm/min scanning speed, and 8 g/min feed rate is considered for multiple-layer deposition.

3.2. Multiple-layer deposition

The five-layer deposition provided a thickness of $\sim 3 \mu\text{m}$. The deposition was characterized for porosity, microhardness, and microstructure.

As mentioned in section 2.3.1, porosity analysis was also carried out on the multi-layer deposition. In this case, the effect of carrier gas flow rate on the porosity could be evaluated as the deposition was carried out under two different flow rates. The cross-section of the multi-layer specimens is shown in Fig. 5. The pores seen in the specimens are circular, indicating porosity due to gas entrapment during the DED process. However, we do not observe any irregular pores, indicating no issues with the fusion during the process (Yadav, Jinoop, et al. 2020; Nayak et al. 2019; Müller et al. 2021). Additionally, the pores were observed closer to the substrate in the first layer of the deposition. The porosity values calculated using Equation 1 for all the specimens were less than 2%, as shown in Fig. 6(a). Furthermore, in the case of specimens 2 and 4, dilution of the substrate into the first layer was observed. This dilution assisted in a better material flow in the first layer, leading to fewer pores. Studies have shown that using constant laser power or decreasing the laser power by 100 W for each layer decreases the possibility of interlayer porosity in the specimens (Yadav, Paul, et al. 2020; Raghavendra et al. 2023).

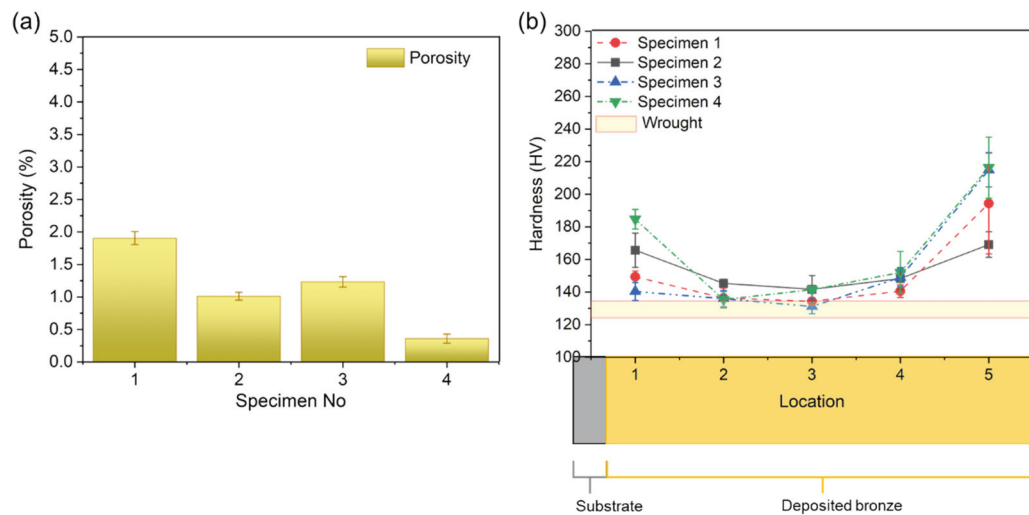


Figure 6 (a) percentage of porosity in the multi-layer specimens (b) microhardness profile

The microhardness analysis of the specimens was carried out at different locations and is represented in Fig. 6(b) and compared with the hardness value of wrought bronze. A slightly higher hardness value is seen than the wrought hardness value in all the locations and specimens. The region closest to the substrate (5 mm from the substrate) has a slightly higher value than the values at 1, 1.5 and 2 mm distance from the substrate. This is due to the rapid cooling rate of the first layer of deposition, which comes into contact with a cold substrate. Additionally, the hardness of specimens 4 and 2 is higher (170 – 185 HV) than specimens 1 and 3 (140 – 150 HV) in the first zone due to the presence of diluted steel particles (Yao et al. 2022). The value stabilizes in the center of the deposition and is in the range of 135 – 150 HV. However, in the topmost layer, an increase in the hardness was observed due to the heat

accumulation from the previous layers and rapid cooling. In this case, specimens 3 and 4, deposited at constant laser power, had a higher hardness than those deposited using decreasing laser power.

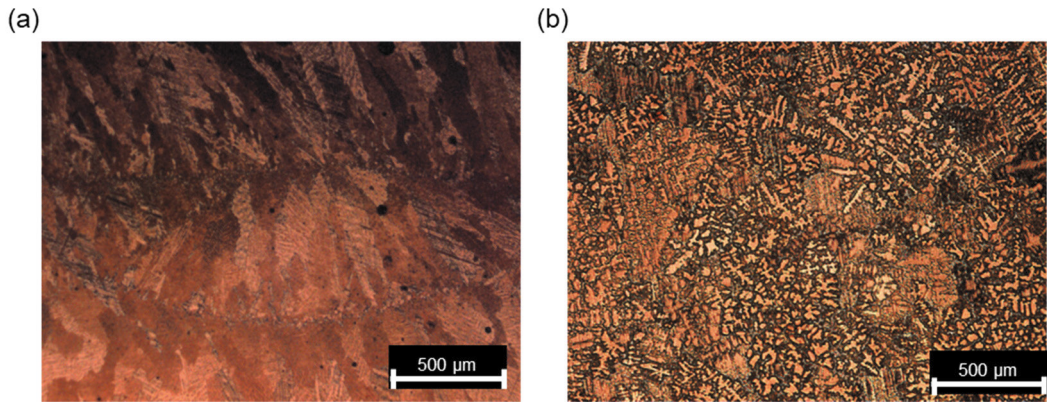


Figure 7 Microstructure of (a) DED bronze indicating columnar grains (b) wrought bronze majorly composed of dendritic phase.

The microstructure of the DED deposited specimen is compared with the wrought bronze in Fig. 7. Fig. 7(a) shows the DED deposited bronze microstructure, mainly consisting of columnar grains oriented in the building and scanning direction. A section of the bead geometry in Fig. 7 (a) shows a clear boundary with small equiaxed grains, which transition into long columnar grains (Liu et al. 2023). On the contrary, the wrought bronze microstructure shown in Fig. 7(b) is uniform dendritic α - δ eutectoid in nature in the entire cross-section. This apparent difference in the microstructure can be attributed to the different manufacturing processes adopted and the thermal gradient involved in the same.

3.3. Wear test

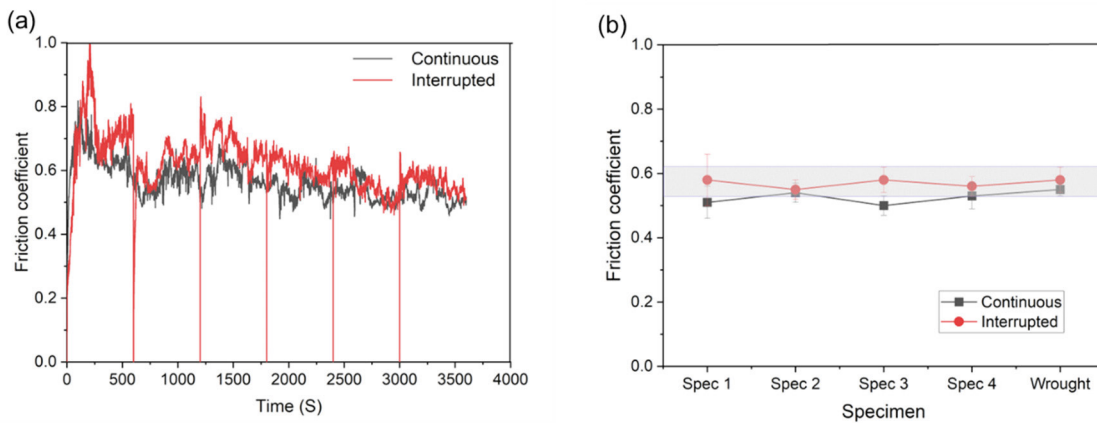


Figure 8 (a) Representative friction coefficient trend for continuous and interrupted wear test (b) average friction coefficient comparison between DED and wrought bronze

The wear test was conducted to compare the friction coefficient of the DED specimens with the wrought specimen and to look for debonding between the substrate and the deposition during the trial. A representative curve of the friction coefficient trend during the test is shown in Fig. 8(a). The curves from the continuous test and the interrupted test overlap towards the end of the test, indicating a stabilization in both cases. The average friction coefficient

indicated in Fig. 8(b) is obtained by considering the steady state section of the friction curve shown in Fig. 8(a). The friction coefficient values are in the range of 0.5 – 0.6 for all the specimens, including the wrought specimens. Similar friction values were obtained for CuSn10 manufactured using DED and tested against a high chromium low carbon steel (Raghavendra et al. 2023). Additionally, forged tin-bronze with Vickers hardness between 250 – 300 HV tested against a GCr15 steel ball yielded a friction coefficient between 0.8 – 0.9(Wei et al. 2022). Therefore, the friction coefficient in the current study is in the acceptable range for dry sliding conditions, considering the hardness values, composition, and counterface material.

4. Conclusion

The study evaluated the possibility of depositing CuSn12Ni2 bronze on a steel substrate. The deposition and characterization of single tracks were carried out to obtain the best process parameter for multi-layer 3 mm thick deposition. Pins were extracted from the multi-layer deposition and tested under dry sliding conditions. The following conclusions were obtained from the study:

- Optimal process parameters with laser power of 2000W, feed rate of 8 g/min, and scanning speed of 800 mm/min were obtained from the single tracks' characterization.
- When depositing at a gas flow rate of 6 L/min, porosity values are significantly reduced near the interface due to the dilution of the substrate.
- Hardness values of the specimens were comparable to or greater than those of wrought bronze, regardless of location.
- Unlike wrought bronze, the DED specimens showcased a columnar grain microstructure instead of a dendritic microstructure.
- The wear test did not induce debonding at the interface, and the friction coefficient between 0.55 – 0.6 obtained was within an acceptable range compared to wrought bronze.

Acknowledgments

This work was financially supported by “**Fondazione Cassa di Risparmio di Trento e Rovereto**” in the framework of the project “18895 - (2021.0561) - Bronze-Worm: Development of an additive manufacturing process for the efficient use of bronze in worm-wheel gearboxes”, call “Bando ricerca e sviluppo 2021/2022”

References

- Ahn, Dong Gyu. 2021. *Directed Energy Deposition (DED) Process: State of the Art. International Journal of Precision Engineering and Manufacturing - Green Technology*. Vol. 8. Korean Society for Precision Engineering. <https://doi.org/10.1007/s40684-020-00302-7>.
- Benedetti, M., A. du Plessis, R. O. Ritchie, M. Dallago, S. M.J. Razavi, and F. Berto. 2021. “Architected Cellular Materials: A Review on Their Mechanical Properties towards Fatigue-Tolerant Design and Fabrication.” *Materials Science and Engineering R: Reports* 144: 100606. <https://doi.org/10.1016/j.mserr.2021.100606>.
- Bruschi, S., R. Bertolini, A. Bordin, F. Medea, and A. Ghiotti. 2016. “Influence of the Machining Parameters and Cooling Strategies on the Wear Behavior of Wrought and Additive Manufactured Ti6Al4V for Biomedical Applications.” *Tribology International* 102: 133–42. <https://doi.org/10.1016/j.triboint.2016.05.036>.
- Crosher, William P. 2002. *Design and Application of the Worm Gear*. ASME Press. <https://doi.org/10.1115/1.801780>.
- Dávila, José Luis, Paulo Inforçatti Neto, Pedro Yoshito Noritomi, Reginaldo Teixeira Coelho, and Jorge Vicente Lopes da Silva. 2020. “Hybrid Manufacturing: A Review of the Synergy between Directed Energy Deposition and Subtractive Processes.” *International Journal of Advanced Manufacturing Technology* 110 (11–12): 3377–90. <https://doi.org/10.1007/s00170-020-06062-7>.
- Duraisamy, R., S. Mohan Kumar, A. Rajesh Kannan, N. Siva Shanmugam, K. Sankaranarayanan, and M. R. Ramesh. 2020. “Tribological Performance of Wire Arc Additive Manufactured 347 Austenitic Stainless Steel under Unlubricated Conditions at Elevated Temperatures.” *Journal of Manufacturing Processes* 56 (November 2019): 306–21. <https://doi.org/10.1016/j.jmapro.2020.04.073>.
- Emminghaus, N, C Hoff, J Hermsdorf, S Kaieler - Lasers in Manufacturing, and undefined 2019. 2019. “Additive Manufacturing of CuSn10

- Powder via Selective Laser Melting.” *Wlt.De*, 1–10. https://www.wlt.de/lim/Proceedings2019/data/PDF/Contribution_187_final.pdf.
- Fontanari, V., M. Benedetti, G. Straffelini, Ch Girardi, and L. Giordanino. 2013. “Tribological Behavior of the Bronze-Steel Pair for Worm Gearing.” *Wear* 302 (1–2): 1520–27. <https://doi.org/10.1016/j.wear.2013.01.058>.
- Liu, Xiao, Haoren Wang, Kevin Kaufmann, and Kenneth Vecchio. 2023. “Directed Energy Deposition of Pure Copper Using Blue Laser.” *Journal of Manufacturing Processes* 85 (November 2022): 314–22. <https://doi.org/10.1016/j.jmapro.2022.11.064>.
- Maconachie, Tobias, Martin Leary, Bill Lozanovski, Xuezhe Zhang, Ma Qian, Omar Faruque, and Milan Brandt. 2019. “SLM Lattice Structures: Properties, Performance, Applications and Challenges6.” *Materials and Design* 183: 108137. <https://doi.org/10.1016/j.matdes.2019.108137>.
- Müller, Vinzenz, Angelina Marko, Tobias Kruse, and Max Biegler. 2021. “Analysis and Recycling of Bronze Grinding Waste to Produce Maritime Components Using Directed Energy Deposition.” *Lasers in Manufacturing Conference 2021*, 1–9.
- Nayak, Saurav K., Sanjay K. Mishra, Christ P. Paul, Arackal N. Jinoop, Sunil Yadav, and Kushvinder S. Bindra. 2019. “Effect of Laser Energy Density on Bulk Properties of SS 316L Structures Built by Laser Additive Manufacturing Using Powder Bed Fusion.” In *ASME 2019 Gas Turbine India Conference*. American Society of Mechanical Engineers. <https://doi.org/10.1115/GTINDIA2019-2452>.
- Onuike, Bonny, and Amit Bandyopadhyay. 2019. “Additive Manufacturing in Repair: Influence of Processing Parameters on Properties of Inconel 718.” *Materials Letters* 252: 256–59. <https://doi.org/10.1016/j.matlet.2019.05.114>.
- Paul, Christ P, Pankaj Bhargava, Atul Kumar, Ayukt K Pathak, and Lalit M Kukreja. 2013. “Laser Rapid Manufacturing: Technology, Applications, Modeling and Future Prospects.” In *Lasers in Manufacturing*, 1–67. John Wiley & Sons, Ltd. <https://doi.org/https://doi.org/10.1002/9781118562857.ch1>.
- Prashanth, K. G., B. Debalina, Z. Wang, P. F. Gostin, A. Gebert, M. Calin, U. Kühn, M. Kamaraj, S. Scudino, and J. Eckert. 2014. “Tribological and Corrosion Properties of Al-12Si Produced by Selective Laser Melting.” *Journal of Materials Research* 89 (3): 2044–54. <https://doi.org/10.1557/jmr.2014.133>.
- Raghavendra, Sunil, Priyadarshini Jayashree, Domenico Antonio Rita, Giuseppe Piras, David Scheider, Marco Chemello, and Matteo Benedetti. 2023. “Wear and Material Characterization of CuSn10 Additively Manufactured Using Directed Energy Deposition.” *Additive Manufacturing Letters* 6 (December 2022). <https://doi.org/10.1016/j.addlet.2023.100136>.
- Wei, Chunhua, Chenglin Niu, Youyuan Tan, and Zhixin Lei. 2022. “Dry-Sliding Tribological Properties of a Tin–Bronze Alloy Produced by Multiaxial Forging and Annealing.” *Industrial Lubrication and Tribology* 74 (6): 692–97. <https://doi.org/10.1108/ILT-01-2022-0014>.
- Yadav, S., A. N. Jinoop, N. Sinha, C. P. Paul, and K. S. Bindra. 2020. “Parametric Investigation and Characterization of Laser Directed Energy Deposited Copper-Nickel Graded Layers.” *International Journal of Advanced Manufacturing Technology* 108 (11–12): 3779–91. <https://doi.org/10.1007/s00170-020-05644-9>.
- Yadav, S., C. P. Paul, A. N. Jinoop, A. K. Rai, and K. S. Bindra. 2020. “Laser Directed Energy Deposition Based Additive Manufacturing of Copper: Process Development and Material Characterizations.” *Journal of Manufacturing Processes* 58 (April): 984–97. <https://doi.org/10.1016/j.jmapro.2020.09.008>.
- Yadav, S., C. P. Paul, A. K. Rai, A. N. Jinoop, S. K. Nayak, R. Singh, and K. S. Bindra. 2022. “Parametric Studies on Laser Additive Manufacturing of Copper on Stainless Steel.” *Journal of Micromanufacturing* 5 (1): 21–28. <https://doi.org/10.1177/25165984211047525>.
- Yao, Chang Liang, Hyun Sung Kang, Ki Yong Lee, Jian Guang Zhai, and Do Sik Shim. 2022. “A Study on Mechanical Properties of CuNi2SiCr Layered on Nickel-Aluminum Bronze via Directed Energy Deposition.” *Journal of Materials Research and Technology* 18: 5337–61. <https://doi.org/10.1016/j.jmrt.2022.04.159>.
- Zykova, A., A. Chumaevskii, A. Vorontsov, K. Kalashnikov, D. Gurianov, A. Gusarova, and E. Kolubaev. 2022. “Evolution of Microstructure and Properties of Fe-Cu, Manufactured by Electron Beam Additive Manufacturing with Subsequent Friction Stir Processing.” *Materials Letters* 307 (September 2021): 131023. <https://doi.org/10.1016/j.matlet.2021.131023>.